

Supplementary Materials: Stacking-Controlled Magnetic Anisotropy

Switching in bilayer Janus $\text{Mn}_2\text{Cl}_3\text{Br}_3$

Table S1. Calculated lattice constant (a), Mn-X-Mn bond angle, Mn-Y-Mn bond angle, and energy difference between FM and Néel AFM for the monolayers $\text{Mn}_2\text{X}_3\text{Y}_3$.

$\text{Mn}_2\text{X}_3\text{Y}_3$	a (Å)	$\angle \text{Mn-X-Mn}$	$\angle \text{Mn-Y-Mn}$	$E_{\text{Néel-AFM}} - E_{\text{FM}}$ (meV)
$\text{Mn}_2\text{Cl}_3\text{Br}_3$	6.32	98.67	88.91	593.16
$\text{Mn}_2\text{Br}_3\text{I}_3$	6.79	95.99	85.97	468.17
$\text{Mn}_2\text{Cl}_3\text{I}_3$	6.60	101.34	80.55	416.81

Table S2. Bilayer $\text{Mn}_2\text{Br}_3\text{I}_3$: theoretical lattice parameter ($a = b$), distance between Mn layers of bilayer Mn-Mn length ($d_{\text{Mn-Mn}}$), energy difference from the ground state (AB-II) $\Delta Z_{\text{X(Y)}} = (Z_{\text{Mn-X(Y)}} - Z_{\text{Mn-X0(Y0)}})/Z_{\text{Mn-X0(Y0)}}$ and MAE.

Stacking configurations	a (Å)	$E - E_0$ (meV)	$d_{\text{Mn-Mn}}$ (Å)	ΔZ_{X}	ΔZ_{Y}	MAE (meV)
AA-II	6.71	36.10	7.281	1.09	-9.25	-39.30
AA-BrI	6.79	60.87	6.744	-0.91/1.24	-5.60/-0.22	-40.13
AA-BrBr	6.67	251.74	5.964	-1.44	-4.41	-33.63
AB-II	6.70	0	7.326	0.41	-4.63	-48.08
AB-BrI	6.71	44.34	6.548	0.55/1.34	-3.53/-3.12	-56.44
AB-BrBr	6.66	184.76	5.959	-0.87	-1.13	-39.12

Table S3. Bilayer $\text{Mn}_2\text{Cl}_3\text{I}_3$: theoretical lattice parameter ($a = b$), distance between Mn layers of bilayer Mn-Mn length ($d_{\text{Mn-Mn}}$), energy difference from the ground state (AB-II), $\Delta Z_{\text{X(Y)}} = (Z_{\text{Mn-X(Y)}} - Z_{\text{Mn-X0(Y0)}})/Z_{\text{Mn-X0(Y0)}}$ and MAE.

Stacking configurations	a (Å)	$E - E_0$ (meV)	$d_{\text{Mn-Mn}}$ (Å)	ΔZ_{X}	ΔZ_{Y}	MAE (meV)
AA-II	6.48	21.40	6.010	1.19	-2.39	-9.21
AA-ClII	6.48	57.82	6.075	-0.54/2.31	-1.81/-0.22	-9.88
AA-ClClI	6.48	180.99	5.914	-0.32	-0.64	-8.12
AB-II	6.47	0	6.815	-0.31	-1.99	-4.97
AB-ClII	6.47	32.98	5.891	-1.43/0.28	-1.87/0.12	-8.37
AB-ClClI	6.48	74.78	5.646	-1.69	-1.08	-8.00

Table S4. MAE for the bilayer MnX_3 (X=Cl, Br, or I) with AA and AB stackings.

Stacking	MnCl_3	MnBr_3	MnI_3
AA	-1.08	-19.36	-30.55

AB	-2.28	-22.90	-34.76
----	-------	--------	--------

Table S5. Interlayer exchange constants of AA/AB-stacking bilayer $\text{Mn}_2\text{Br}_3\text{I}_3$

Stacking configurations	J_{inter}^{1x} (meV)	J_{inter}^{2x} (meV)	J_{inter}^x (meV)	J_{inter}^{1z} (meV)	J_{inter}^{2z} (meV)	J_{inter}^z (meV)
AA-BrBr	4.52	0.09	4.78	4.77	0.15	5.22
AA-ClBr	2.83	0.08	3.06	3.03	0.02	3.10
AA-ClCl	1.72	0.01	1.75	1.68	0.02	1.75
AB-BrBr	3.98	0.33	2.99	4.01	0.28	2.86
AB-ClBr	2.23	0.27	1.93	2.00	0.26	1.79
AB-ClCl	1.03	0.15	0.95	0.88	0.13	0.84

Table S6. Interlayer exchange constants of AA/AB-stacking bilayer $\text{Mn}_2\text{Br}_3\text{I}_3$

Stacking configurations	J_{inter}^{1x} (meV)	J_{inter}^{2x} (meV)	J_{inter}^x (meV)	J_{inter}^{1z} (meV)	J_{inter}^{2z} (meV)	J_{inter}^z (meV)
AA-II	0.58	0.01	0.62	0.81	-0.11	0.47
AA-BrI	3.95	1.30	7.85	3.52	1.00	6.52
AA-BrBr	0.59	-0.04	0.47	0.53	-0.03	0.43
AB-BrBr	0.03	0.01	0.05	-0.04	-0.01	-0.06
AB-BrI	0.25	0.23	0.81	0.20	0.16	0.57
AB-BrBr	0.15	0.09	0.34	0.08	0.11	0.36

Table S7. Intralayer exchange parameters, interlayer exchange parameters of z and x directions and the anisotropy between the z and x directions (ΔJ_{intra} and ΔJ_{inter}) of AA/AB-stacking bilayer $\text{Mn}_2\text{Br}_3\text{I}_3$.

Stacking configurations	J_{intra}^x (meV)	J_{inter}^x (meV)	J_{intra}^z (meV)	J_{inter}^z (meV)	ΔJ_{intra} (meV)	ΔJ_{inter} (meV)
AA-II	1.58	0.62	0.45	0.47	-1.14	-0.15
AA-BrI	3.18	7.85	2.01	6.52	-1.17	-1.34
AA-BrBr	1.31	0.47	0.31	0.43	-1.00	-0.04
AB-BrBr	1.41	0.05	0.16	-0.06	-1.25	-0.12
AB-BrI	1.57	0.81	0.12	0.57	-1.45	-0.24
AB-BrBr	1.53	0.34	0.39	0.36	-1.14	0.02

Table S8. Interlayer exchange constants of AA/AB-stacking bilayer $\text{Mn}_2\text{Cl}_3\text{I}_3$

Stacking configurations	J_{inter}^{1x} (meV)	J_{inter}^{2x} (meV)	J_{inter}^x (meV)	J_{inter}^{1z} (meV)	J_{inter}^{2z} (meV)	J_{inter}^z (meV)
AA-II	0.19	0.09	0.47	0.25	0.19	0.83

AA-CII	0.23	0.07	0.45	0.22	0.10	0.52
AA-ClCl	0.09	0.00	0.08	0.20	0.09	0.48
AB-II	-0.01	-0.02	-0.06	0.07	-0.17	-0.48
AB-CII	0.03	0.20	0.60	0.03	0.18	0.56
AB-ClCl	0.01	0.02	0.08	0.01	0.01	0.05

Table S9. Intralayer exchange parameters, interlayer exchange parameters of z and x directions and the anisotropy between the z and x directions (ΔJ_{intra} and ΔJ_{inter}) of AA/AB-stacking bilayer $Mn_2Cl_3I_3$

Stacking configurations	J_{intra}^x (meV)	J_{inter}^x (meV)	J_{intra}^z (meV)	J_{inter}^z (meV)	ΔJ_{intra} (meV)	ΔJ_{inter} (meV)
AA-II	0.53	0.47	0.29	0.83	-0.25	0.36
AA-CII	0.67	0.45	0.41	0.52	-0.26	0.07
AA-ClCl	0.50	0.08	-0.11	0.48	-0.61	0.40
AB-II	0.38	-0.06	0.14	-0.48	-0.23	-0.43
AB-CII	0.16	0.60	-0.23	0.56	-0.39	-0.05
AB-ClCl	0.53	0.08	0.30	0.05	-0.23	-0.03

Table S10. Intralayer exchange parameters, interlayer exchange parameters of z and x directions and the anisotropy between the z and x directions (ΔJ_{intra} and ΔJ_{inter}) of AA/AB-stacking bilayer MnX_3

Stacking configurations	J_{intra}^x (meV)	J_{inter}^x (meV)	J_{intra}^z (meV)	J_{inter}^z (meV)	ΔJ_{intra} (meV)	ΔJ_{inter} (meV)
AA-MnCl ₃	4.40	1.89	5.29	3.38	0.89	1.49
AB-MnCl ₃	2.09	0.14	2.12	0.27	0.03	0.13
AA-MnBr ₃	4.34	2.18	3.68	2.86	-0.66	0.68
AB-MnBr ₃	3.86	1.56	3.32	1.54	-0.54	-0.01
AA-MnI ₃	2.28	1.01	1.62	1.03	-0.65	0.02
AB-MnI ₃	2.13	0.18	1.53	0.09	-0.60	-0.09

Table S11 MAE of Janus monolayers and bilayer $Mn_2Cl_3Br_3$ under AA-BrBr stacking with $U= 3.3, 3.6,$ and 3.9 eV.

Structures	MAE (meV)		
	$U= 3.3$ eV.	$U= 3.6$ eV.	$U= 3.9$ eV.
Monolayer $Mn_2Cl_3Br_3$	-5.06	-5.32	-5.75
AA-BrBr bilayer $Mn_2Cl_3Br_3$	2.17	2.39	2.49

Table S12. ΔA_{ij} between the monolayer and the top layer in the AA-YY stacked bilayer for different $Mn_2X_3Y_3$ systems.

$Mn_2X_3Y_3$	ΔA_{11} (1/eV)	ΔA_{12} (1/eV)	ΔA_{13} (1/eV)
$Mn_2Cl_3Br_3$	277.79	-305.75	-288.13
$Mn_2Br_3I_3$	322.47	-285.75	-691.37
$Mn_2Cr_3I_3$	20.85	-101.18	82.57

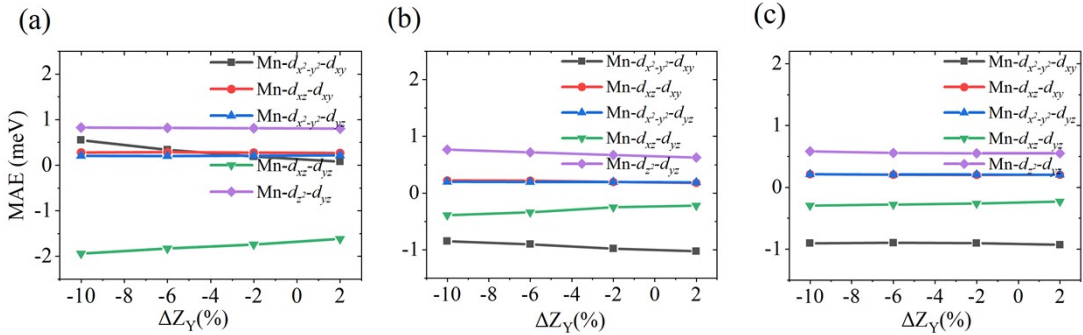


Figure S1 Effect of the reduction in the distance between the Y layer and the Mn layer on orbital-resolved MAE of Mn- d orbitals in (a) $Mn_2Cl_3Br_3$, (b) $Mn_2Br_3I_3$, and (c) $Mn_2Cl_3I_3$.

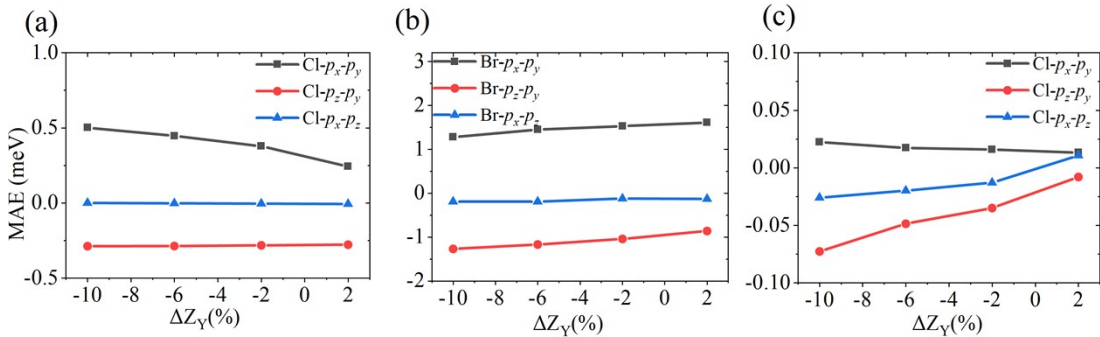


Figure S2 Effect of the reduction in the distance between the Y layer and the Mn layer on orbital-resolved MAE of X- p orbitals in (a) $Mn_2Cl_3Br_3$, (b) $Mn_2Br_3I_3$, and (c) $Mn_2Cl_3I_3$.

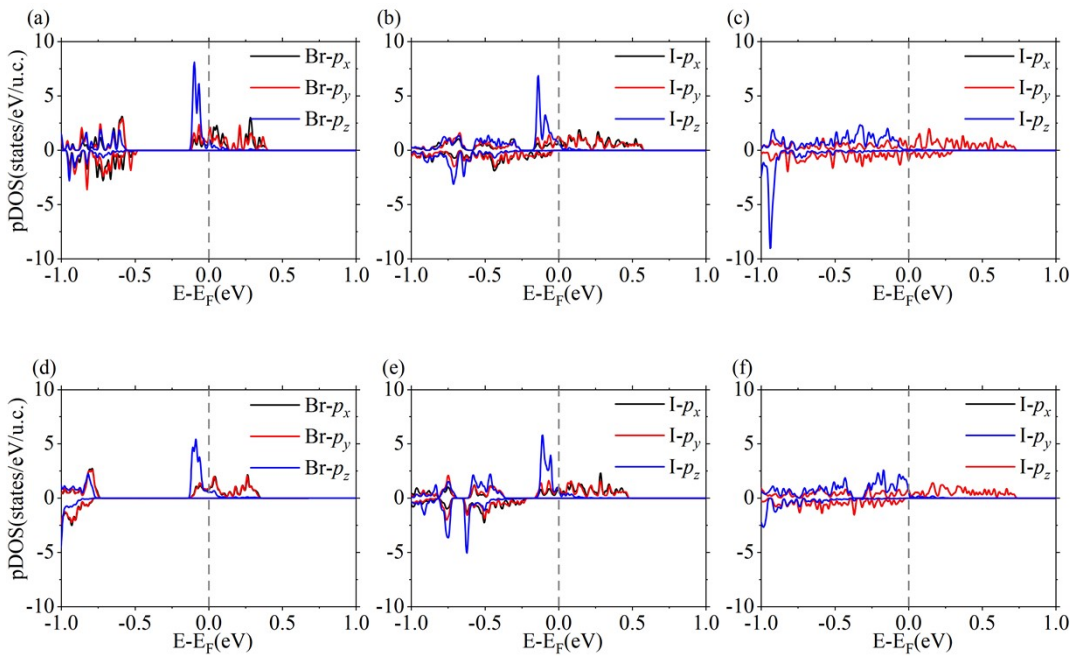


Figure S3 PDOS of the monolayers (a) $\text{Mn}_2\text{Cl}_3\text{Br}_3$, (b) $\text{Mn}_2\text{Br}_3\text{I}_3$, and (c) $\text{Mn}_2\text{Cl}_3\text{I}_3$. PDOS of one layer from AA-YY stacking bilayer of (d) $\text{Mn}_2\text{Cl}_3\text{Br}_3$, (e) $\text{Mn}_2\text{Br}_3\text{I}_3$, and (f) $\text{Mn}_2\text{Cl}_3\text{I}_3$.

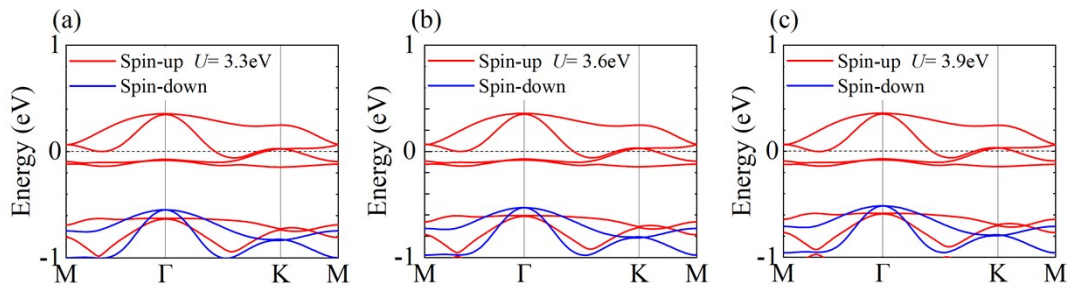


Figure S4 Spin-polarized band structures of the $\text{Mn}_2\text{Cl}_3\text{Br}_3$ monolayer at $U=$ (a) 3.3, (b) 3.6, and (c) 3.9 eV.

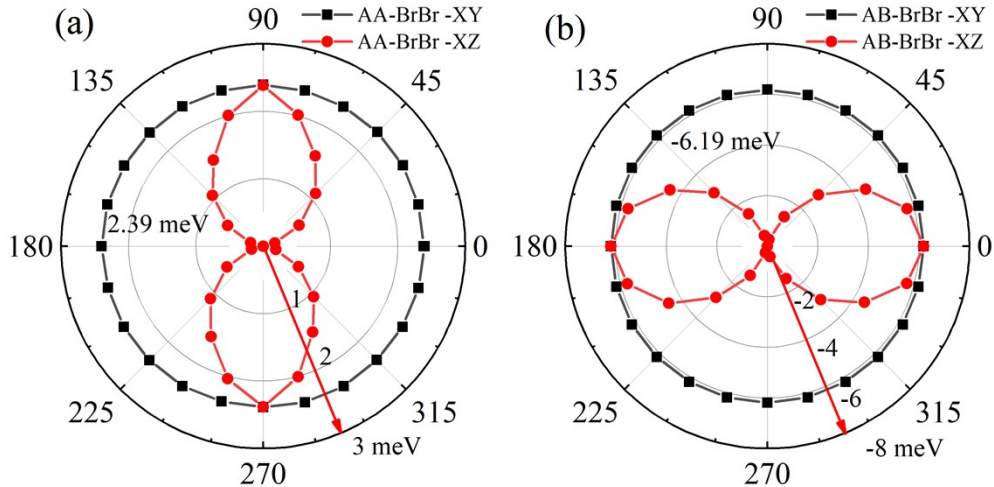


Fig S5 MAE with spin rotation of bilayer $\text{Mn}_2\text{Cl}_3\text{Br}_3$ under (a) AA-BrBr and (b) AB-BrBr stacking order.